International Journal of Basic and Applied Chemical Sciences ISSN: 2277-2073 (Online)
An Open Access, Online International Journal Available at http://www.cibtech.org/jcs.htm
2018 Vol. 8(1) January-March, pp.13-30/Shukla et al.
Research Article

BIO-MIMETIC OXOVANADIUM (IV) COMPLEXES OF ISONIAZID SCHIFF BASE: SPECTROSCOPIC CHARACTERIZATION, DFT STUDY, ANTIBACTERIAL SCREENING AND *IN-VITRO* ANTIDIABETIC ACTIVITY WITH INHIBITION OF PANCREATIC α- AMYLASE

[*]S. N. Shukla, P. Gaur, S. Jhariya, B. Chaurasia, P. Vaidya and D. Dehariya
[1]Coordination Chemistry Research Lab, Department of Chemistry, Government Science College, Jabalpur (M.P.) 482001, India
**Author for Correspondence*

ABSTRACT
In present investigation two Schiff base ligands were synthesized by condensation of isonicotinylhydrazide with benzaldehyde/ *p*-chlorobenzaldehyde and their four oxovanadium (IV) complexes were prepared. Ligands and complexes were characterized by elemental analysis, molar conductance, magnetic moment, electronic spectroscopy, FTIR, ^{1}H-NMR and ^{13}C-NMR. DFT study was employed to optimize the geometry of the investigated compounds. Using molecular modeling, bond lengths, bond angles, molecular electrostatic potential map (MEP), and Mullikan charge were also evaluated. The Schiff base ligands and complexes have been investigated for antidiabetic activity. The *in-vitro* antidiabetic results suggest that complexes exhibit prominent antidibetic activity. Ligand and complexes were also screened for their antibacterial activity against gram-negative bacteria ***Escherichia coli*** in comparison to standard drugs. All complexes were found more potent than Schiff base ligands. The MIC of complexes was also studied.

Keywords: *Schiff Base; Molecular Modeling; Type 2 Diabetes; α- Amylase; Antibacterial Activity*

INTRODUCTION
Vanadium (IV) compounds have been shown to exhibit a wide range of biomimetic activities, including the inhibition of enzymes and insulin mimetics, (Zhang, *et al.*, 2017; Sahani MK, *et al.*, 2014). Numerous *in vitro* and *in vivo* studies have shown that vanadium has insulin like effects in the liver, skeletal muscle and adipose tissue as well as improves hepatic and muscle insulin sensitivity in type 2 diabetes **(**Samy M. El-Megharbel *et al*, 2015). A few vanadium compounds seem to have insulin-enhancing effects, and among others, *bis*(picolinato)oxidovanadium (IV) has proved to be orally active in treating diabetes mellitus. However, other two complexes namely *bis*(maltolato)oxidovanadium (IV) and *bis*(ethylmaltolato)oxidovanadium (IV) have also shown significant glucose lowering effect (Isaac Z. Gundhla *et al.*, 2014).
Schiff base and their complex derivatives have fascinated researchers in last twenty five year due to its vivid applications. Ligands with O and N donor atoms have played an important role in coordination chemistry and recently, considerable attention has been paid, due to their stability, biological activity and potential applications in many fields such as oxidation catalysis, electrochemistry etc (Shukla *et al.*, 2015; Liu *et al.*, 1996; Djebbar *et. al.*, 1998; Hamada, 1997). Isoniazid is an antibacterial, which is very active against microorganism. Schiff bases derived from isoniazid; act as O and N donor bidentate ligands to stabilize 5-coordinated square pyramidal oxovanadium (IV) complexes (Shivakumar *et al*., 2012).
Therefore, in anticipation of good reactivity and biological activity we have synthesized two Schiff base ligands of isonicotinylhydrazide and its four complexes with vanadyl sulphate. We have characterized compounds by spectroscopic technique and to explore *in vitro* antidiabetic activity complexes have been tested *in-vitro* for pancreatic alpha-amylase inhibition activity. Since, density functional theory (DFT) has been accepted as a powerful tool in optimization of molecular structure and providing a lot of information about structural properties (Shoba *et al*., 2011; Tyagi *et al.*, 2015), we are also interested in DFT study of compounds.

MATERIALS AND METHODS

Benzaldehyde, *p*-chlorobenzaldehyde (CDH), isonicotinylhydrazide (Lancaster, U.K.), vanadyl sulphate (E. Merck), enzyme alpha-amylase, muller hinton agar media (Himedia) were purchased and used as received. AR grade methyl alcohol, ethyl alcohol, acetonitrile, acetone, dimethylsulphoxide were used throughout the experiment. FTIR spectra were recorded in KBr pallets on Shimadzu–8400S FTIR spectrophotometer in the range 4000–400 cm^{-1}. Electronic absorption spectra were recorded in the range 800-200 nm with EI - 2305, double beam spectrophotometer equipped with a PC. ^{1}H–NMR and ^{13}C-NMR spectrum was recorded with Bruker Avance 700 (FT NMR). The ESI spectra were recorded on Agilent 6520 (QTOF) Mass spectrophotometer. Elemental analyses (C, H and N) were performed on Elementar Vario EL III, elemental analyzer. Molar conductance was measured in DMSO with an EI-181 digital conductivity bridge with dipping type of cell at 25°C. The metal content was analyzed gravimetrically by the literature procedure (Jeffery *et al.* 1989).

Synthesis of Schiff base Ligands

Preparation of (Z)-N'- benzylideneisonicotinohydrazide, ***(SBBZINH); L_1:***

This ligand was prepared according to literature procedure (Mehrotra *et al*., 2011). Isonicotinohydrazide (1.37 g, 0.01 mol) was dissolved into 25 mL methanol in a two neck flask. Benzaldehyde (1.01 mL, 0.01 mol) mixed into 25 mL of methanol was added to above reaction mixture. The reaction mixture was kept under reflux in an inert atmosphere. Progress of reaction was observed by TLC. After 10 h, reaction mixture was concentrated and kept at room temperature for slow evaporation. After two days an off white precipitate was separated, which was filtered off, washed with sodium bisulphite, vacuum dried and recrystallized from ethanol. Colour = off white; Yield: 1.90 g (80%); m.p. = 180 °C; Found: C, 69.20; H, 4.88; N, 18.60; **$C_{13}H_{10}N_3O$** ($M\tau$ = 225.09). Required: C, 69.32; H, 4.92; N, 18.66. Selected infrared absorption (KBr, cm^{-1}): ν(N-H), 3200(w); $\nu(C=O)_{CONH}$, 1685(s); $\nu(C=N)_{cyclic}$, 1615(sh); $\nu(HC=N)_{imine}$, 1599(s). Electronic spectra (λ_{max} in nm (ε in (mol L^{-1} cm^{-1})) in DMSO: 240(360), 280(120), 320(200). ^{1}H-NMR (700 MHz; δ, DMSO-d_6): δ 12.487(s,1H, –CONH); 8.731 - 8.751 (m, 2H, pyridyl-H); δ 8.366(s, 1H,–CH=N); 7.847-7.896 (m, 2H, pyridyl-H);δ 7.419-7.840 (m, 5H, Ar–H). ^{13}C{^{1}H}-NMR (700 MHz; δ, DMSO-d_6) δ 164.74(CH=N); δ 142.60-152.07 (pyridyl -C); δ 123.31–135.38(Ar–C). ESI-Mass spectra, m/z: $[C_8H_7N_2O + H^+]^+$ = 147.05, $[C_7H_6N_3O + H^+]^+$ = 148.056, $[C_{13}H_{10}N_3O]^+$ = 224.08, $[C_{13}H_{11}N_3O + H^+]$ = 226.06; $M\tau$ = 225.09.

Preparation of (E)-N'-(4-chlorobenzylidene)isonicotinohydrazide, ***(SBCBZINH);L_2:***

Isonicotinohydrazide (1.37g, 0.01 mol) was dissolved into 25 mL methanol in a two neck flask. *p*-Chlorobenzaldehyde (1.20 mL, 0.01 mol) mixed into 25 mL of methanol was added to above reaction mixture. The reaction mixture was kept under reflux for 15 h in an inert atmosphere. Progress of reaction was observed by TLC. After completion, reaction mixture was concentrated and kept at room temperature for slow evaporation. After two days, a white precipitate was separated, which was filtered off, washed with sodium bisulphite, vacuum dried and recrystallized from ethanol. Colour = White, Yield: 2.065 g (75%); m.p. = 190 °C. Found: C, 60.09; H, 3.84; N; 16.10. **$C_{13}H_{10}ClN_3O$** ($M\tau$ = 259.05). Required: C, 60.12; H, 3.88; N, 16.18. Selected infrared absorption (KBr, cm^{-1}): ν(N-H), 3220(w); $\nu(C=O)_{CONH}$, 1668(s); $\nu(C=N)_{cyclic}$, 1616(s); $\nu(HC=N)_{imine}$, 1605(sh). Electronic spectra (λ_{max} in nm (ε in (mol L^{-1} cm^{-1})) in DMSO: 225(410), 258(245), 330(130). ^{1}H-NMR (700 MHz; δ, DMSO-d_6): δ12.477(s,1H, –CONH); 8.741-8.753 (m, 2H, pyridyl-H); δ8.367 (s, 1H,–CH=N); 7.857-7.886 (m, 2H, pyridyl-H); δ7.418-7.830 (t,5H, Ar–H).^{13}C{^{1}H}-NMR (700 MHz;δ, DMSO-d_6) δ 164.65(CH=N); δ 141.61-153.08 (pyridyl -C); δ 124.30–134.37(Ar–C). ESI-Mass spectra, m/z: $[C_8H_7N_2O + H^+]^+$ = 147.05, $[C_7H_6N_3O + H^+]^+$ = 148.056, $[C_6H_4N_3Cl]^+$ = 111.00, $[C_6H_5N_2O]^+$ = 121.04, $[C_7H_5Cl\ N_2]^+$ = 138.00, $[C_7H_6N_3O]^+$ = 148.05, $[C_7H_6ClN_2]^+$ = 153.03 , $[\ C_8H_6ClN_2O\ ]^+$ = 181.01, $[C_{13}H_{10}ClN_3O]^+$ = 224.08, $[C_{13}H_9N_3OCl\ ]^+$ = 258.04, $[\ C_{13}H_{10}ClN_3O + H^+\ ]$ = 260.06; $M\tau$ = 259.05.

Synthesis of complexes:

*$[VO(SBBZINH)(H_2O)_2]SO_4$, Complex **1***:

$VOSO_4 \cdot 5H_2O$ (0.253 g, 0.01 mmol) dissolved in minimum amount of water and recrystallized Schiff base (0.225 g, 0.01 mmol) were mixed in 20 mL of methanol. The reaction mixture was kept under stirring for 2 h in an inert atmosphere. The colour of solution changes from dark yellow to dark green. Thereafter, reaction mixture was refluxed for 7 h. After reduction of volume by slow evaporation a green colour solid was precipitated, which was filtered off, washed with diethyl ether, dried under vacuum and recrystallized from methanol. Colour = Green, Yield: 0.366 g (76%); m. p. 250 °C. Found: C, 36.75; H, 3.50; N, 9.80; V, 11.96; **$C_{13}H_{15}N_3O_8SV$** ($M\tau$ = 424.28). Required: C, 36.80; H, 3.56; N, 9.90; V, 12.01; Selected infrared absorption (KBr, cm^{-1}): ν(N-H), 3150(w); $\nu(CO)_{CONH}$, 1650(s); $\nu(C=N)_{cyclic}$,1600(s); $\nu(HC=N)_{imine}$, 1550(sh)); ν(M=O), 960(sh); $\delta(H_2O)$, 760(sh). Electronic spectra (λ_{max} in nm (ε in (mol L^{-1} cm^{-1})) in DMF: 355(225), 425(85). μ_{eff} = 1.68 B.M. Molar conductance Λ_m at 25 °C (Ω^{-1} cm^2mol^{-1}): 80 in DMF. ESI-Mass spectra, *m/z*: $[C_{13}H_{11}N_3O + H^+]^+$ = 226.09; $[C_{13}H_{15}N_3O_8\ SV + H^+]^+$ = 425.28; Mτ = 424.28.

*$[VO(SBBZINH)_2]SO_4$, Complex **2**:*

$VOSO_4 \cdot 5H_2O$ (0.253g, 0.01mmol) dissolved in minimum amount of water and recrystallized Schiff base (0.450 g, 0.02 mmol) were mixed in 20 mL of methanol. The reaction mixture was kept under stirring for 1 h in an inert atmosphere. The colour of solution changes from yellow to greenish brown. Thereafter, reaction mixture was refluxed for 5 h. After reduction of volume by slow evaporation a brownish green colour solid was precipitated, which was filtered off, washed with diethyl ether, dried under vacuum and recrystallized from ethanol.

Colour = Brownish green, Yield: 0.545 g (77%); m. p. 280 °C. Found: C, 50.70; H, 3.57; N, 13.45; V, 8.18; **$C_{26}H_{22}N_6O_7SV$** ($M\tau$ = 613.5). Required: C, 50.90; H, 3.61; N, 13.70; V, 8.30; Selected infrared absorption (KBr, cm^{-1}): ν(N-H), 3090(w); $\nu(CO)_{CONH}$, 1635(s); $\nu(C=N)_{cyclic,}$ 1604(s); $\nu(HC=N)_{imine}$, 1554(sh)); ν(M=O), 974(sh). Electronic spectra (λ_{max} in nm (ε in (mol L^{-1} cm^{-1})) in DMF: 360(100), 460(90). μ_{eff} = 1.61 B.M. Molar conductance Λ_m at 25 °C (Ω^{-1} cm^2mol^{-1}): 107 in DMF. ESI-Mass spectra, *m/z*: $[C_{13}H_{11}N_3O + H^+]^+$ = 226.09; $[C_{26}H_{22}N_6O_7SV^{2+} + H^+]^+$ = 614.07; Mτ; = 613.5.

$[VO(SBCBZINH)(H_2O)_2]SO_4$, Complex **3**:

$VOSO_4 \cdot 5H_2O$ (0.253 g, 0.01 mmol) dissolved in minimum amount of water and recrystallized Schiff base (0.259 g, 0.01 mmol) were mixed in 20 mL of methanol. Few drops of sodium hydroxide was added to catalyze the reaction and the reaction mixture were kept under stirring for 2 h in an inert atmosphere. The colour of solution changes from dark yellow to green. Thereafter, reaction mixture was refluxed for 6 h. After reduction of volume by slow evaporation a light green colour solid was precipitated, which was filtered off, washed with diethyl ether, dried under vacuum and recrystallized from methanol. Colour = Light green, Yield: 0.308 g (61%); m. p. 270 °C. Found: C, 34.00; H, 3.01; N, 9.11; V, 10.99; **$C_{13}H_{14}N_3O_8SV$** ($M\tau$ = 458.73). Required: C, 34.04; H, 3.08; N, 9.16; V, 11.11; Selected infrared absorption (KBr, cm^{-1}): ν(N-H), 3160(w); $\nu(CO)_{CONH}$, 1655(s); $\nu(C=N)_{cyclic}$,1610(s); $\nu(HC=N)_{imine}$, 1570(sh)); ν(M=O), 940(sh); $\delta(H_2O)$, 755(sh). Electronic spectra (λ_{max} in nm (ε in (mol L^{-1} cm^{-1})) in DMF: 365(200), 470(80). μ_{eff} = 1.70 B.M. Molar conductance Λ_m at 25 °C (Ω^{-1} cm^2mol^{-1}): 90 in DMF. ESI-Mass spectra, *m/z*: $[C_{13}H_{10}\ ClN_3O + H^+]^+$ = 260.05, $[C_{13}H_{14}\ ClN_3O_8\ SV + H^+]^+$ = 459.73, Mτ = 458.73.

*$[VO(SBCBZINH)_2]SO_4$, Complex **4***:

$VOSO_4 \cdot 5H_2O$ (0.253 g, 0.01 mmol) dissolved in minimum amount of water and recrystallized Schiff base (0.518 g, 0.02 mmol) were mixed in 25 mL of methanol. The reaction mixture kept under stirring for 1 h in an inert atmosphere. The colour of solution changes from yellow to brown. Thereafter, reaction mixture was refluxed for 5 h. After reduction of volume by slow evaporation a dark green colour solid was precipitated, which was filtered off, washed with diethyl ether, dried under vacuum and recrystallized from methanol. Colour = Dark green, Yield: 0.575 g (74%); m. p. 290°C. Found: C, 45.67; H, 2.90; N, 12.20; V, 7.40 **$C_{26}H_{20}N_6O_7SV$** ($M\tau$ = 682.39). Required: C, 45.76; H, 2.95; N, 12.32; V, 7.47; Selected

infrared absorption (KBr, cm^{-1}): ν(N-H), 3085(w); $\nu(CO)_{CONH}$, 1642(s); $\nu(C=N)_{cyclic,}$ 1610(s); $\nu(HC=N)_{imine}$, 1552(sh)); ν(M=O), 935(sh). Electronic spectra (λ_{max} in nm (ε in (mol L^{-1} cm^{-1})) in DMF: 370(150), 450(95). μ_{eff} = 1.65 B.M. Molar conductance Λ_m at 25 °C (Ω^{-1} cm^2mol^{-1}): 110 in DMF. ESI-Mass spectra, *m/z*: $[C_{13}H_{10}ClN_3O + H^+] = 260.06$; $[C_{26}H_{20}Cl_2N_6O_7\,SV + H^+]^+ = 683.39$, Mτ = 682.39.

Computational Analysis:

To understand structure of the ligands and complexes, the DFT calculations were performed by Gaussian 09 software using the B3LYP parameter density function, which includes Becke's gradient exchange correction with the Lee, Yang, Parr correlation functional (Becke 1993; Lee *et al.*, 1988). Full geometry optimization of the ligands and its complexes was carried out using density functional theory (DFT) method of B3LYP with 6-311++G(d,p) and/or 3-21+G* basic set for all nonmetallic atoms and Los Alamos National Laboratory 2 double zeta (LANL2DZ) basic set for the central metal atoms in gas phase (Maurya *et al.* 2014). The optimized structures, HOMO–LUMO and Mulliken charges, are presented and discussed. The quantum chemical parameters such as separation energies (Δ*E*), Mulliken electronegativity (χ), dipole moment, absolute hardness (η), absolute softness (*σ*), chemical potential (*Pi*), global softness (*S*), global electrophilicity (ω), additional electronic charge (ΔN_{max}), dipole moment (μ) and total energy (ETD-HF/ETDKS) were calculated after geometrical optimization of the structures of all compounds.

Biological Studies

Antidiabetic activity

The effect of α-amylase (EC 3.2.1.1) activity was determined according to the method described in literature (Silavwe *et al.,* 2015) with some modification. Preliminary experiments were conducted to establish optimal assay conditions such as temperature, substrate enzyme and inhibitor concentration. The antidiabetic activity was investigated through the inhibition of α-amylase, an enzyme active in the digestion of starch, which thus reduces the absorption of glucose. Briefly 1 mL of each complex (dissolved in DMSO) was taken in pre-labeled test tubes. A volume of 20 µL of α-amylase was added to each test tube and incubated for 10 min at 37 °C. After the incubation 2 mL acetate buffer was added to each test tube, thereafter, 200 µL of 1% starch solution was added to each test tube and the mixture was reincubated for 1 h at 37 °C. Then 200 µL of 1% iodine solution was added to each test tube. Absorbance of the mixture was taken at 540 nm. Sample, substrate and α-amylase blank were undertaken under the same conditions. Percent α-amylase inhibition was determined by the following equation:

$$\%\ \alpha - \text{amylase inhibition} = \frac{\text{Absorbance of Control} - \text{Absorbance of Complex}}{\text{Absorbance of control}}\ \text{X}\ 100$$

Antibacterial study

All ligands and its metal complexes were screened for antibacterial activity against gram negative bacteria *Escherichia coli* (ATCC no. 13522) at different concentration. Agar well diffusion method was used for antibacterial screening (Pelczar *et al,* 2001; Shukla *et al*., 2008). The culture media were prepared by mixing 1 g of agar and 2.8 g of nutrient agar in 100 mL of water in a sterile conical flask and stirred for 15 min to make sure complete suspension. The media was autoclaved at 15 psi pressure at 120°C for 15 min and poured into a sterilized petri plate and allowed to settle. The bacterial culture was inoculated and spread homogeneously over the media. The inoculants were prepared by 4–5 similar colonies of *Escherichia coli*. In the particular inoculants petri plate the 0.05 mL of 5 mM (dissolved in DMSO) solutions of the compounds were added to each well with the help of micropipette. These plates were incubated at 37±1 °C for 24 – 48 hours in refrigerated incubator shakers. The results in the form of zone inhibition were measured in mm. No inhibition zone was observed around the well in the control but ligands and complexes show inhibition zone formations around the well.

Minimum inhibitory concentration (MIC)

In order to observe the activity and confirm the sensitivity, all ligands and complexes were tested for minimum inhibitory concentration (MIC). The most popular method for MIC evaluation, successive dilution method was used (Mazzola *et al.,* 2009). MIC is concentration of the higher dilution tube, in which bacterial growth was absent.

RESULTS AND DISCUSSION

Characterization of Ligands

The elemental analysis data for the synthesized ligands, **(SBBZINH)** and **(SBCBZINH)** were in full agreement with the proposed empirical formula.

FT-IR Spectra of Ligands

FTIR of both ligands, **(SBBZINH) /L_1** and **(SBCBZINH) / L_2** exhibit a sharp and strong band due to ν(HC=N) of the azomethine group at 1599 cm^{-1} and 1605cm^{-1} respectively, conforming the formation of Schiff base (Biradar *et al.*, 1984; Abd-Elzaher 2001). Both ligands exhibit two bands at 3350-3200 cm^{-1} assigned for symmetric and asymmetric ν(N-H). Signals at ~ 1685 cm^{-1} and 1615 cm^{-1} were assigned to ν(CO) of CONH moiety and cyclic ν(C=N). FT-IR spectra of ligand **L_1** is shown in figure 1**.**

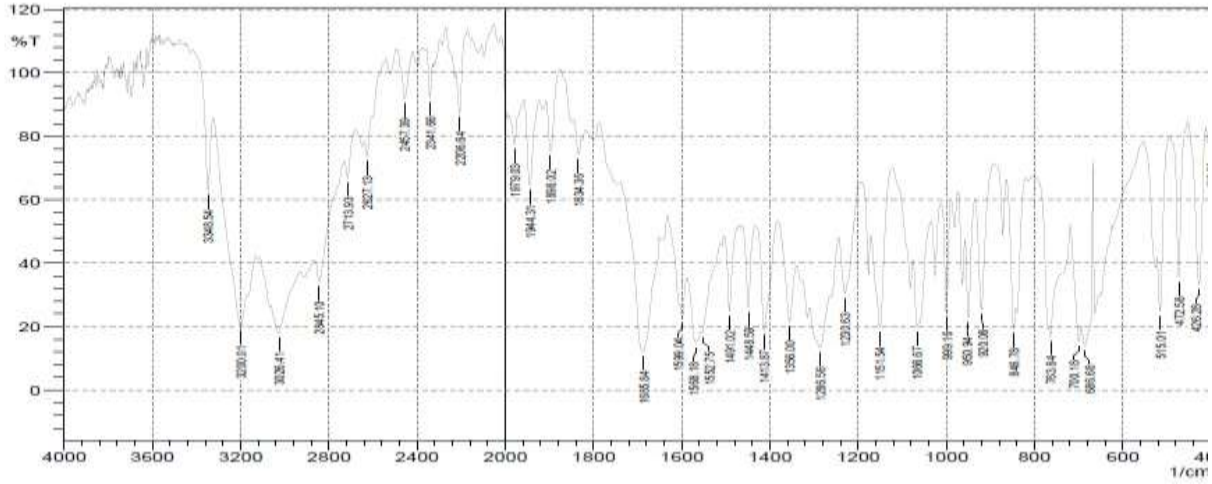

Figure 1: FT-IR spectra of SBBZINH

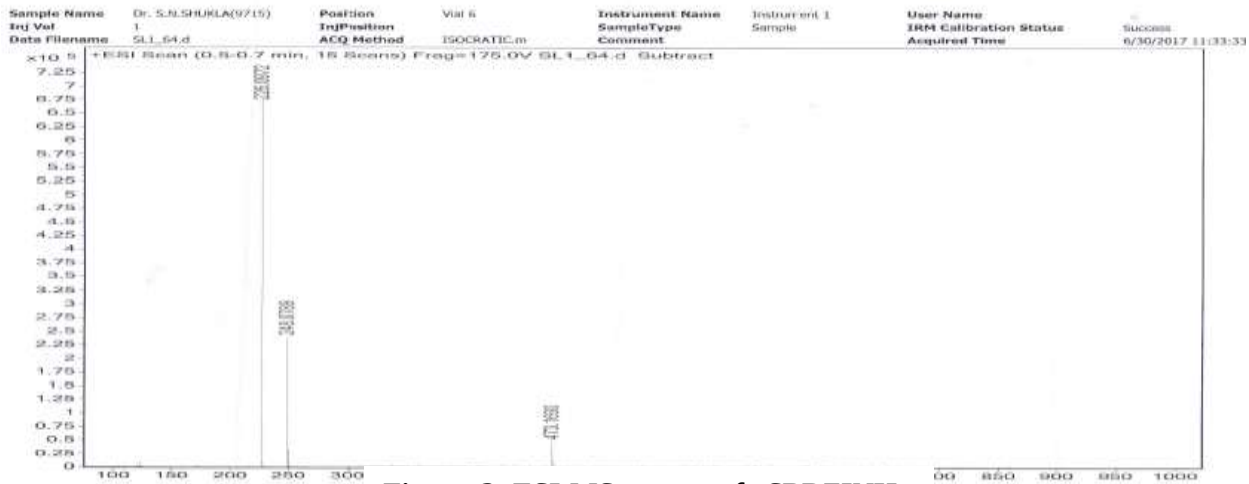

Figure 2: ESI-MS spectra of SBBZINH

ESI-MS Spectra of Ligands

ESI-Mass spectra of ligands exhibit several peaks depending upon the fragmentation pattern. Isotopic pattern of molecular ion peak gave clear evidence about molecular mass. An ESI-Mass spectrum of

SBBZINH, displayed in **Fig. 2** shows a strong pseudo molecular ion peaks in ESI-MS at *m/z* = 226.06, attributed for $[C_{13}H_{10}N_3O+ H^+]^+$, confirming its molecular weight. Similarly, ESI-Mass of ligand **SBCBZINH** also shows a pseudo molecular ion peak at *m/ z* = 260.06, attributed for $[C_{13}H_{10}ClN_3O +H^+]^+$ confirming its molecular weight.

UV-VIS Spectra of Ligands

The electronic spectra (**fig. 3**) of Schiff base **SBBZINH** in Free State exhibit three bands at ~240 nm, ~280 nm and 320 nm. The first band was assigned to $\pi \rightarrow \pi^*$ transition of C=C transition. However, other two bands were assigned to $n \rightarrow \pi^*$ transition associated with transfer of lone pair situated at N and O of C=N and C=O groups respectively. Electronic spectra of **SBCBZINH** exhibit three bands at about 225nm, ~258 nm and 330 nm. First band associated $\pi \rightarrow \pi^*$ transition of C=C transition and other two bands were attributed to $n \rightarrow \pi^*$ transitions.

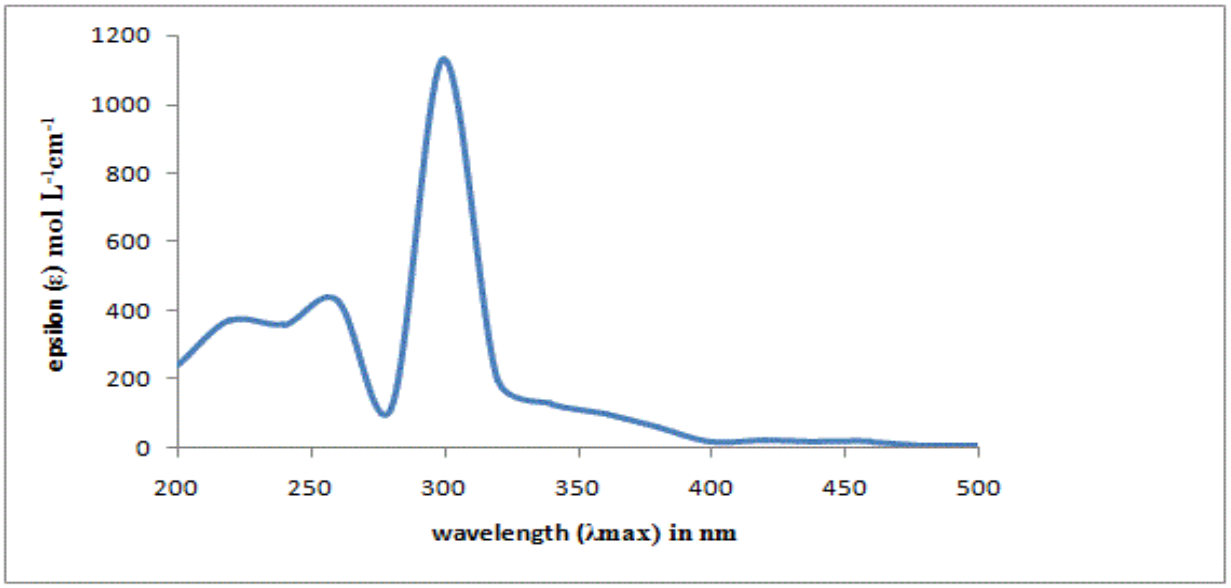

Figure 3: UV-VIS spectra of SBBZINH

^{1}H-NMR Spectra of Ligands

^{1}H-NMR of ligands shows a signal between δ 8.366 - 8.387 ppm assigned for one azomethine (>CH=N) proton. In **SBBZINH** two doublets centered at δ 8.748 ppm and δ 8.733 ppm for two protons were assigned for pyridyl proton (H_1, H_2). Signals for another two pyridyl protons was appeared as double doublets between δ 7.815 -7.847 ppm. A multiplets δ 7.419 - 7.461 ppm for three protons was attributed for three aromatic protons (H_7, H_8 and H_9) of benzene ring. Two doublets appeared between δ 7.859-7.896 ppm for two protons were assigned for two aromatic protons. ^{1}H-NMR of **SBCBZINH** exhibit a multiplet between δ 7.418 - 7.830 ppm for four protons was attributed to four aromatic protons. A

multiplet between δ 8.741 - 8.753 ppm was attributed for four protons of pyridyl protons. A singlet observed at ~ δ 12.477 in both ligands was attributed for CONH protons.

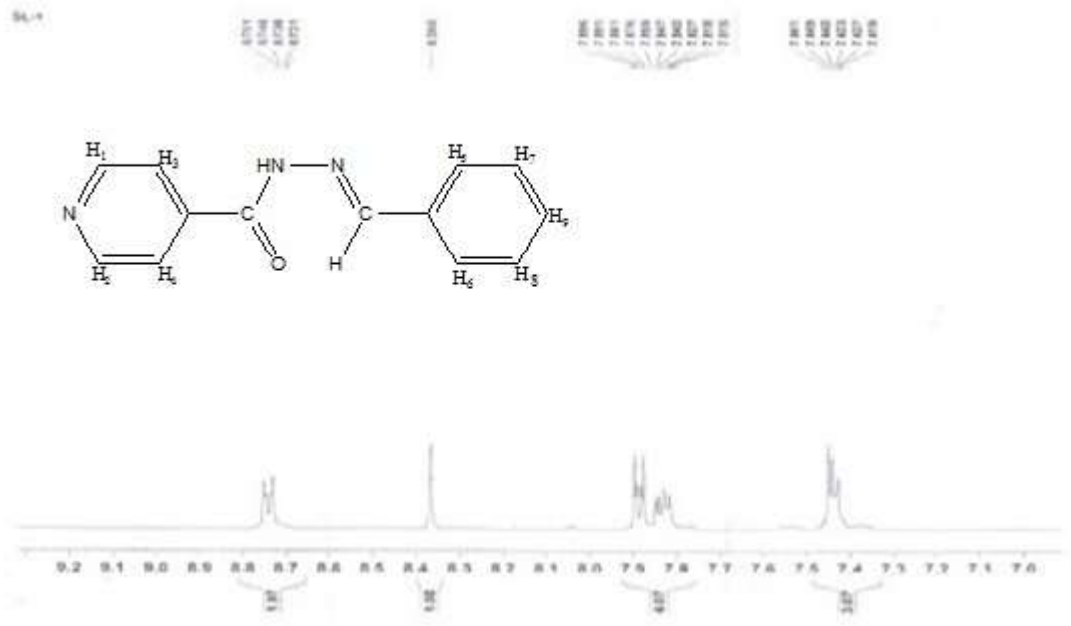

Figure 4: ^{1}H spectra of SBBZINH

^{13}C-NMR Spectra of Ligands

In ^{13}C-NMR, the number of signals represents the number of carbons of the compound which are chemically non-equivalent. ^{13}C-NMR spectra of **SBBZINH** exhibit a signal at about δ 164.74 ppm assigned for -CH=N carbon. Pyridyl carbon display signals between δ 142.60-152.07 ppm. The signals observed at δ 123.31-135.38 ppm were assigned for aromatic carbon. ^{13}C-NMR of **SBCBZINH** exhibit signals at about *δ* 124.30–134.37ppm were assigned for aromatic carbon. The signals observed between δ 141.61-153.08ppm attributed for pyridyl carbon. A signal at about δ 164.65ppm assigned for -CH=N carbon.

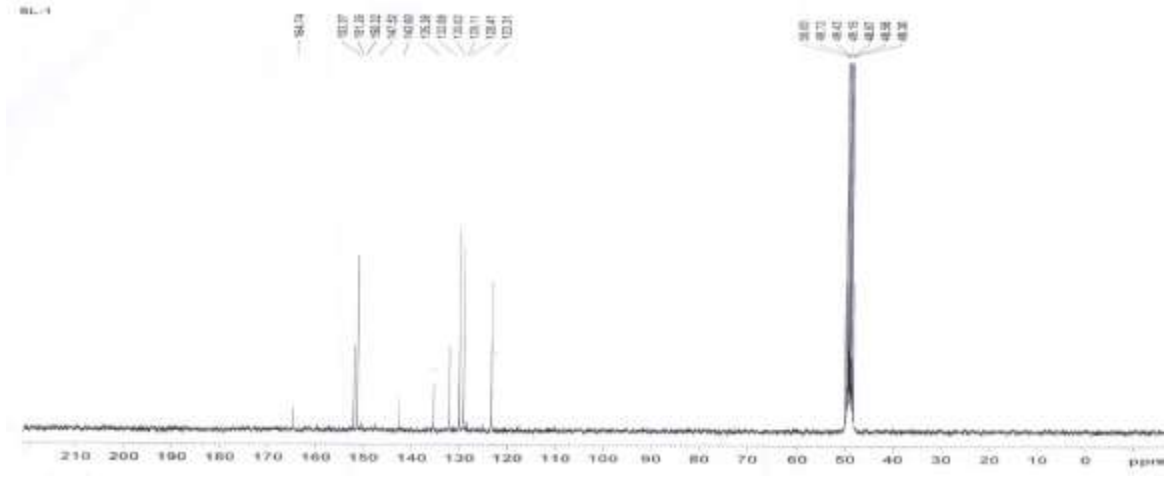

Figure 5: ^{13}C spectra of SBBZINH

Thus on the basis of C, H, N analyses, ESI-MS, FT-IR, ^{1}H-NMR and ^{13}C-NMR most probable structure of the ligands were suggested as below in Figure 6 - 7.

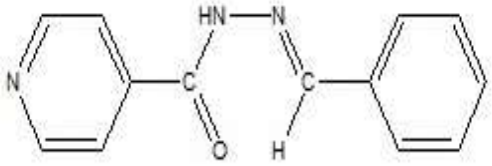

Figure 6: Chemical structure of SBBZINH

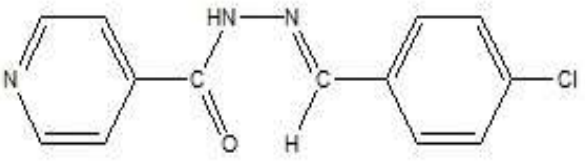

Figure 7: Chemical structure of SBCBZINH

Characterization of Complexes

The stoichiometries of the complexes were in agreement with elemental analyses. The molar conductance observed in between 80–110 $\Omega^{-1}cm^2mol^{-1}$ in 10^{-3} molar DMF solution of these complexes, consistent with the 1: 1 electrolytic nature of the complexes (Geary 1971). The presence of sulfate ion outside coordination sphere was checked qualitatively by using saturated solution of barium (II) chloride.

$[(VO\ (SBBZINH)_2)SO_4\ ]\ [\ DMF] \rightarrow [VO\ (SBBZINH)_2]^{2+} + SO_4^{2-}$

At room temperature, the observed value of the magnetic moments for the present complexes is in the range 1.61–1.70 BM, as expected for paramagnetic as S = 1/2 with a dxy based ground state (Sachin and Narayan 2012). These data suggest that the complexes under this investigation are mononuclear and paramagnetic (Dutta and Syamal 1993).

FT-IR Spectra of Complexes

In FTIR of complexes the peak observed at ~ 1600 cm^{-1} in ligands for azomethine group, was shifted to lower frequency (cal. 30 – 40cm^{-1}) and appeared at 1554 cm^{-1} indicating coordination of azomethine nitrogen with VO^{+2} metal ion (R Amit YAUL *et.al.*,2014). The spectra of all oxovanadium (IV) complexes show a new characteristic band around 940–974 cm^{-1} due to ν(V=O) vibrations. A signal exhibit in complexes **1** and **3** at about 760 and 755 cm^{-1} respectively was attributed for wagging and rocking mode of coordinated water. The presence of ionic sulfate in complex was confirmed by appearance of bands in 1130-1057 cm^{-1} and 570-645 cm^{-1}. FT-IR spectra of complex **2**, is given in figure 8.

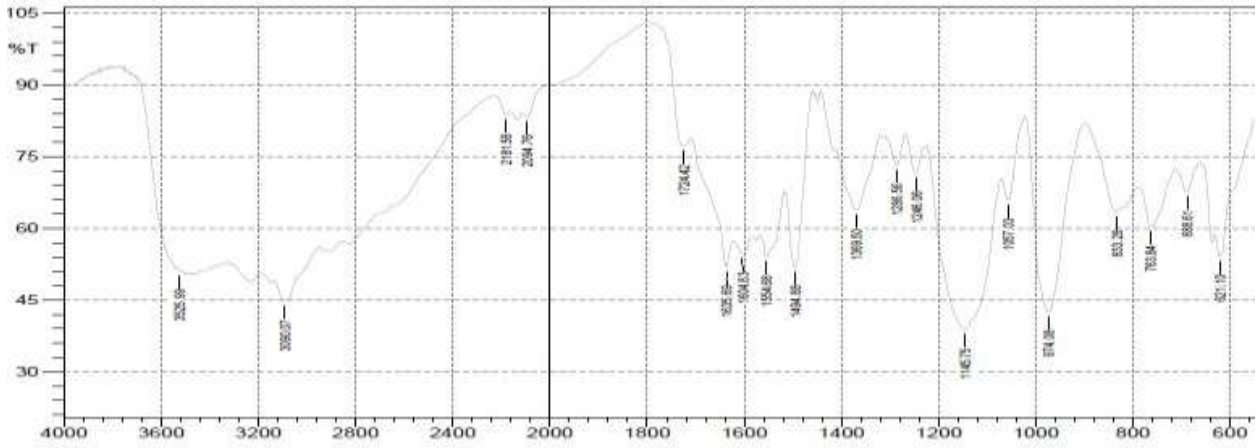

Figure 8: FT-IR spectra complex 2

ESI-MS Spectra of Complexes

ESI-Mass spectra of all four complexes exhibit several peaks depending upon the fragmentation pattern. Isotopic pattern of molecular ion peak gave clear confirmation about molecular mass. The ESI-MS spectra of complexes exhibits pseudo molecular ion peaks for $[L + H^+]^+$; $[M^{2+} + HSO4^-]^+$. ESI-MS of complex **2** is given in **Fig. 9.** It shows peaks at about *m/z* = 226.09 and 614.07 attributed for $[C_{13}H_{11}N_3O + H^+]^+$; and $[C_{26}H_{22}N_6O_7SV^{2+} + H^+]^+$. The peak at *m/z* = 614.07 was pseudo molecular ion peak suggesting molecular weight of complex.

Research Article

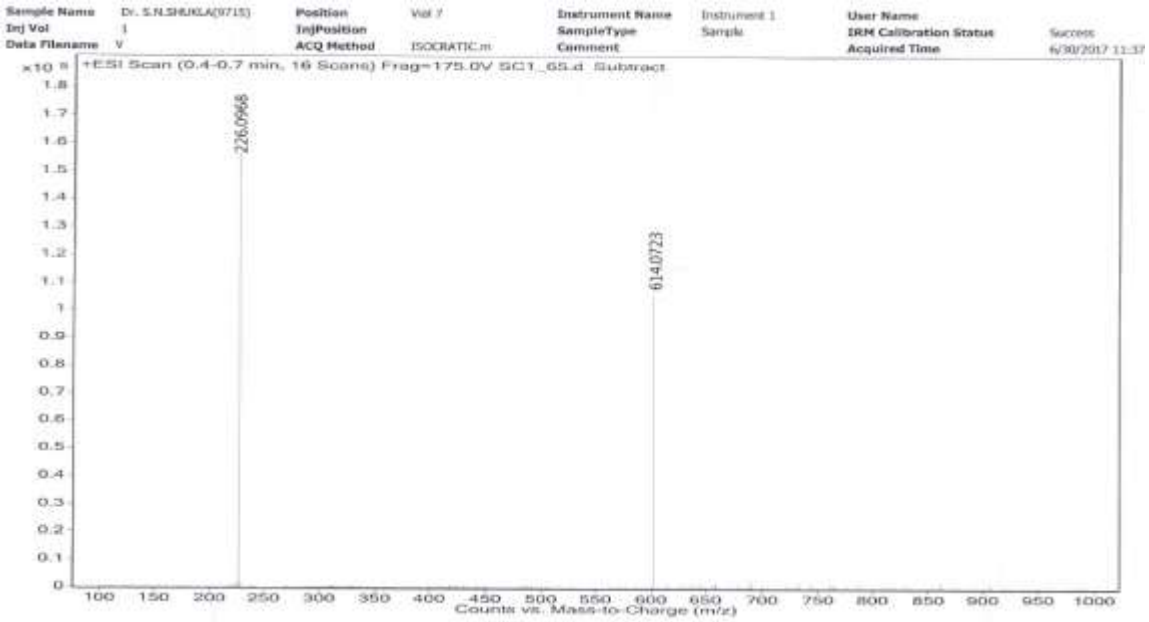

Figure 9:. ESI-MS of complex 2

The electronic spectra of all the compounds were recorded in 10^{-3} molar DMF solution in the range 200–800 nm. The electronic spectra of ligand exhibit three bands between 240 nm, 280 nm and 320 nm that is due to $\pi \rightarrow \pi^*$, $n \rightarrow \pi^*$ and $n \rightarrow \pi^*$ associated with C=C, C=N and C=O transitions. In complex **1** appearance of a low energy band in the 360 nm, may be assigned for ligand to metal charge transfer transition (Balakrishnan and Neelakantan 2017). Complex **1, 2, 3** and complex **4** display a weak broad band at the range of 430- 460 nm, expected for d–d transition $[(dxy \rightarrow d_{x2-y2});(^2B_2 \rightarrow {}^2B_1)]$, suggesting that five coordinated oxo vanadium (IV) complexes. Electronic spectra of complex **2** is given in figure 10.

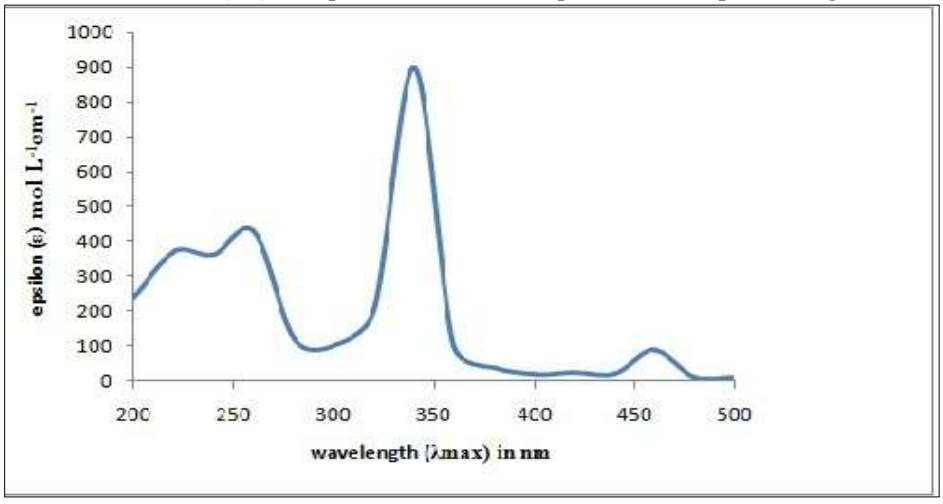

Figure 10: UV-VIS spectra of complex 2

Computational Analysis

Geometrical parameters

In order to investigate the structure of ligand and complexes, time dependent density functional theory (TD-DFT) calculations were done using Gaussian 09 software. Geometrical parameters such as bond length, bond angle and dihedral angle of optimized structure are reported in table 1. In ligand SBBZINH

the calculated bond lengths of C(14)=N(12)$_{azomethine}$, C(13)=O(25), H(26)-N(11) and C(03)-C(04)$_{pyridyl\ ring}$ are 1.293, 1.258, 1.300 and 1.395 respectively. Similarly, computed bond angles in **SBBZINH** are C(14)-N(12)-N(11), C(14)-C(28)-C(15), C(13)-O(25)-N(11) and H(07)-C(02)-C(03) are in 119.999°, 129.990°, 120.000° and 25.510° respectively. V(57)=O(58), V(57)–O(17) and V(57)–N(13)$_{azomethine}$ in the present complex **2** are 1.638, 1.868 and 1.895 Å respectively. The significant computed bond angles in the complex **2** for N(13)–V(57)–O(17), O(17)–V(57)–O(58), C(11)–N(13)–N(14), N(42)–V(57)–N(13), N(42)–V(57)–O(17) and O(45)–V(57)–N(13) are 78.822°, 122.734°, 123.169°, 6.906°, 87.527° and 105.328° respectively. Various bond lengths, bond angles and dihedral angles generated from the optimized structure of the ligand **SBBZINH** and **complex 2** are given in **table 1**.

Frontier molecular orbitals analysis

The HOMO is the orbital that primarily acts as an electron donor and the LUMO largely acts as the electron acceptor and the energy gap between HOMO and LUMO set apart the chemical stability of molecule (Mir *et el.,* 2017). Two important molecular orbitals, highest occupied molecular orbital and lowest unoccupied molecular orbital have been calculated for ligand **SBBZINH** and complex **2**. The value of HOMO and LUMO for **SBBZINH** are -0.25175 a.u. and -0.09030 a.u. respectively, which is displayed in **Fig. 11(a)**. However for **Complex 2** the value of HOMO and LUMO are -0.10600 a.u. and -0.07331 a.u. respectively as displayed in **Fig. 11(b)**. The energy gaps (ΔE) between for ligand is 0.16145 a.u. while in complexes, the energy gap is 0.03269 a.u.

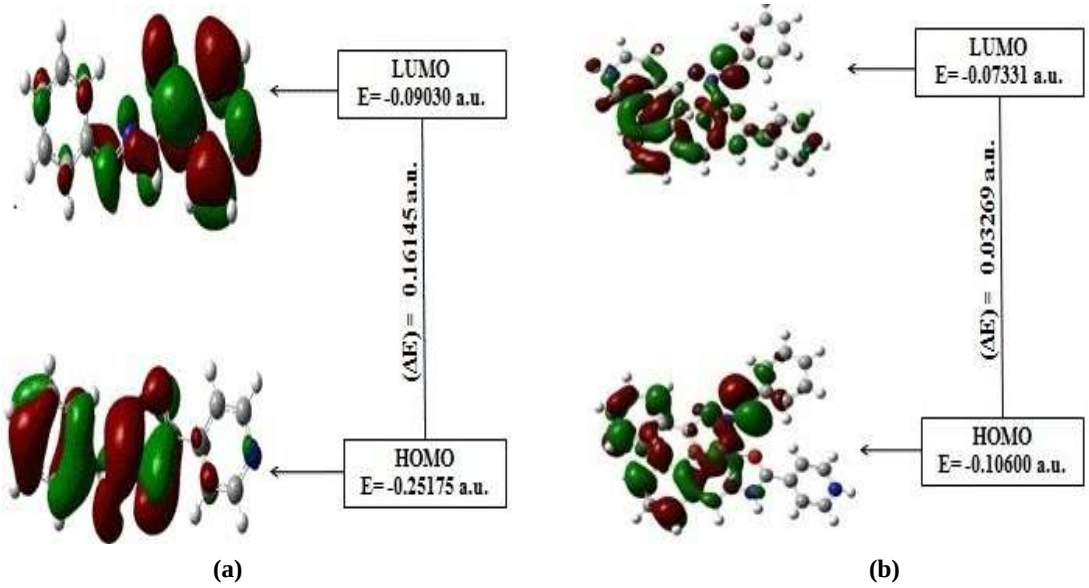

Figure.11 (a) HOMO–LUMO structure with energy-level diagram of **SBBZINH** (b) **[VO(SBBZINH)$_2$]SO$_4$**

The calculated energies of the highest occupied molecular orbital (HOMO) and lowest unoccupied molecular orbital (LUMO) shows that:

1. The energy of the frontier orbitals for molecules in terms of ionization energy (IE) and electron affinity (IA) of the **SBBZINH** and its complex.
2. There is a very short gap between HOMO and LUMO in complex as compared with ligand. This result suggests high reactivity of complex.
3. Complex exhibit high value of the dipole moment, which may favors it dipole-dipole interactions with high dipole moment species, mainly in biological systems.

Table 1: Selected geometrical parameters of Ligand 1 and Complex 2

Ligand 1		Complex 2	
Bond Connectivity	**Bond Length (in Angstrom)**	**Bond Connectivity**	**Bond Length (in Angstrom)**
$C(14)=N(12)_{azomethine}$	1.293	$C(11)=N(13)_{azomethine}$	1.310
C(13)=O(25)	1.300	C(16)=O(17)	1.271
H(26)-N(11)	1.258	$V(57)=O(58)_{oxo}$	1.638
$C(03)-C(04)_{pyridyl\ ring}$	1.395	$V(57)–O(17)_{amide}$	1.868
$N(10)-C(01)_{\ pyridyl\ ring}$	1.343	$V(57)–N(13)_{azomethine}$	1.895
$C(16)-C(17)_{benzene\ ring}$	1.401	V(57)–O(45)	1.868
		V(57)–N(42)	1.895

Ligand 1		Complex 2	
Bond Connectivity	**Bond Angle (in degrees)**	**Bond Connectivity**	**Bond Angle (in degrees)**
C(14)-N(12)-N(11)	119.999	N(13)–V(57)–O(17)	78.822
C(14)-C(28)-C(15)	129.990	O(17)–V(57)–O(58)	122.734
C(13)-O(25)-N(11)	120.000	C(11)–N(13)–N(14)	123.169
H(07)-C(02)-C(03)	25.510	N(42)– V(57)–N(13)	6.906
$C(01)-N(10)-C(05)_{\ pyridyl\ ring}$	29.267	N(42)–V(57)–O(17)	87.527
H(24)-C(19)-C(20)	120.000	O(45)–V(57)–N(13)	105.328

Ligand 1		Complex 2	
Bond Connectivity	**Dihedral Angle (in degrees)**	**Bond Connectivity**	**Dihedral Angle (in degrees)**
H(25)-N(11)-N(12)-C(14)	90.000	C(44)-O(45)-V(57)-O(58)	90.404
O(24)-N(11)-N(12)-C(13)	30.000	O(17)-C(16)-C(19)-C(18)	-178.790
H(25)-N(11)-N(12)-C(14)	-180.000	N(43)-N(42)-V(57)-O(58)	-104.152
O(24)-N(11)-H(25)-C(13)	-150.000	O(45)-V(57)-O(17)-C(16)	-119.107
O(24)-C(13)-N(11)-H(25)	-150.000	N(42)-V(57)-N(13)-C(11)	-137.440

Quantum chemical parameters

The calculated values of quantum chemical parameters such as Mulliken electronegativity (χ), dipole moment, chemical potential (Pi), global hardness (η), global softness (S), global electrophilicity (ω), absolute softness (σ) and electronic charge (ΔN_{max}) were listed in **Table 2.**

Table 2: Quantum chemical parameters of SBBZINH and Complex 2

Compound (eV)	Total energy (a.u.) E(TD-HF/TD-KS)	Dipole moment (debye)	χ (eV)	η(eV)	σ (eV)	Pi (eV)	$S(eV^{-1})$	ω(eV)	ΔN_{max}
SBBZINH	-741.510	5.567	0.171	0.080	12.387	-0.171	6.193	0.181	2.118
Complex 2	-1628.109	6.11	0.089	0.016	61.180	-0.089	30.590	0.245	5.485

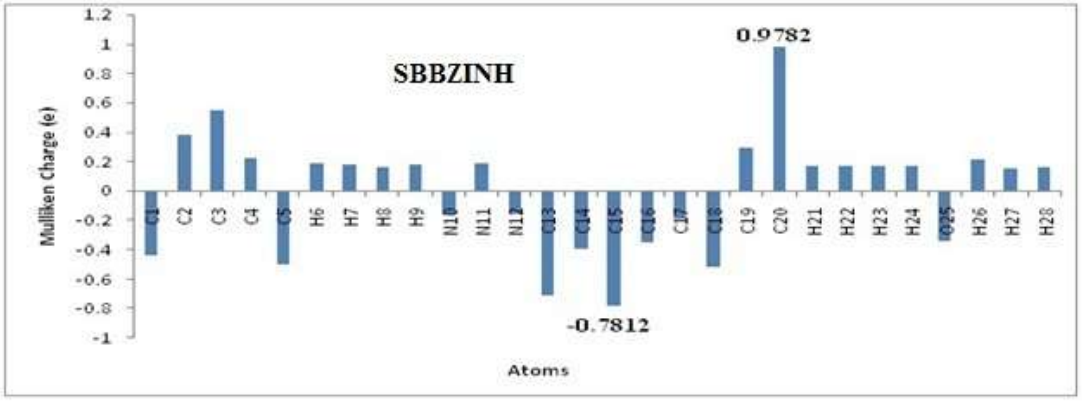

Figure 12: Mulliken atomic charge plot of SBBZINH

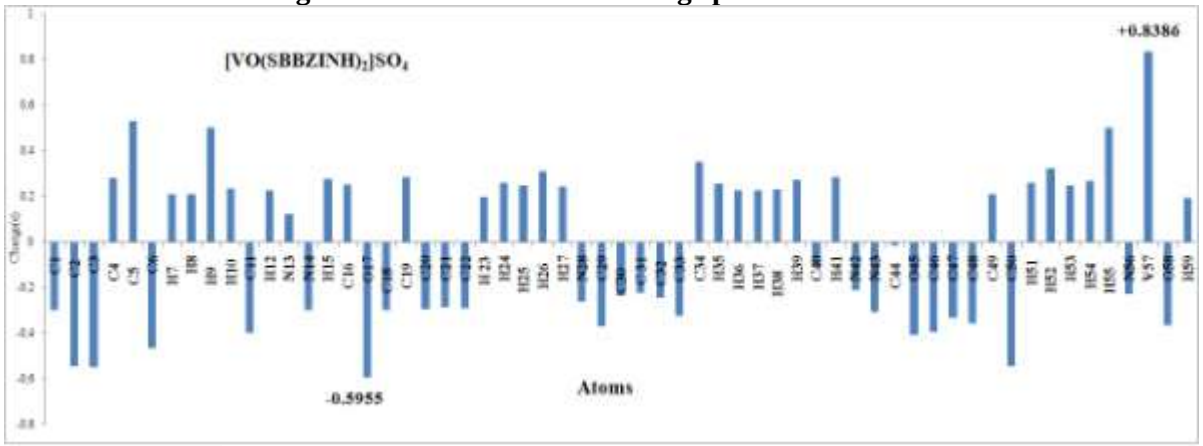

Figure 13: Mulliken atomic charge plot of Complex 2

On the basis of above data we can conclude that:

1. **SBBZINH** coordinates to vanadium (IV) through azomethine nitrogen and oxygen of the (CONH) group.
2. The increase in the value of global electrophilicity (ω) in complex indicates higher electron accepting capability.
3. The negative values of chemical potential (*Pi*) in complex indicate that energy decrease during complex formation due to accepting electronic charge form **SBBZINH**.
4. The energy difference between values of absolute softness (σ) in **SBBZINH,** indicating a good tendency of chelation with metal ions.

Mulliken atomic charge analysis

The Mulliken population analysis of **SBBZINH** and **Complex 2** were done by using method B3LYP/6-311++G(d,p) and LANL2DZ basis set in gas phase. The Mulliken charge is directly related to the vibrational properties of the molecule and indicates how the positive and negative charges present in a molecule increase or decrease the bond length. The illustration of atomic charges for **SBBZINH** and its complex is shown as bar diagram and figure. The result shows that, in **SBBZINH** more positive charges on C3 (+0.5456) and C20 (+0.9782) carbon atoms because these atoms are associated to more electronegative oxygen and nitrogen atom. On the other hand, in case of **Complex 2** vanadium ion possesses higher positive charge of (+0.8386) for that reason, more electronegative two imine nitrogen atoms of **SBBZINH** as well as two electronegative oxygen atoms can coordinated with metal center. This result is consistent with the molecular electrostatic potential (Balachandran and Parimala 2012). The Mulliken atomic charge of ligand **SBBZINH** and **Complex 2** are shown in Figure **12-13**.

Molecular Surface electrostatic potential analysis (MSEP) and contour maps

The molecular surface electrostatic potential (MSEP) surface diagram is used to understand the reactive behavior of a molecules, negative regions can be regarded as nucleophilic centers, whereas the positive regions are potential electrophilic sites. The MSEP of **SBBZINH** and its complex are shown in **(Fig. 14).** The negative regions are mainly over the oxygen atoms (deep red/yellow) on -CONH groups and nitrogen atoms of –CONH and -C=NH- (imine) groups. The hydrogen and carbon atoms bear the maximum region of positive charge and the most positive regions (blue/green) are observed around the hydrogen atoms of C–H groups as well as carbon atoms of imine groups. The color codes of this map are in the ranges between –0.098 a.u. (deep red) to +0.098 a.u. (deep blue) in the **SBBZINH**. In case of **Complex 2 (Fig. 15)** map are in the range –0.090 a.u. to +0. 090 a.u. The different values of the electrostatic potential at the surface are represented by different colors (Raj *et al.*, 2015).

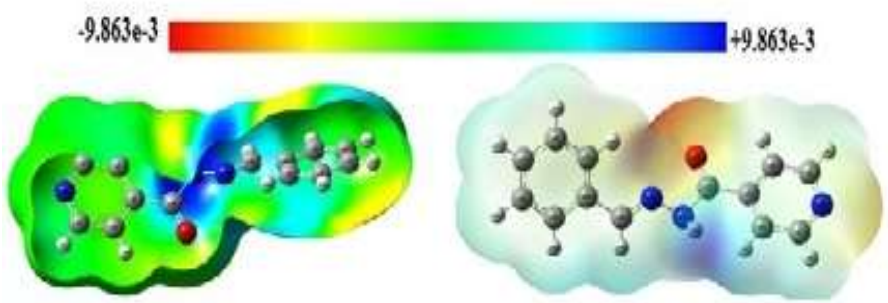

Figure 14: Molecular Surface Electrostatic Potential (MSEP) of SBBZINH

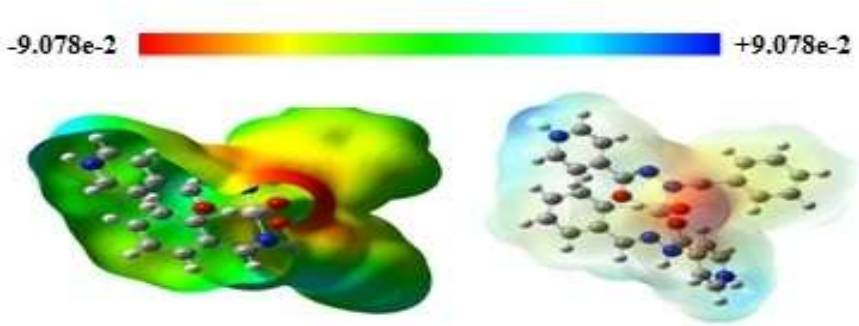

Figure 15: Molecular Surface Electrostatic Potential (MSEP) of Complex 2

On the basis of elemental analyses, molar conductance, magnetic susceptibility, ESI-MS, FT-IR, electronic spectra and DFT calculation most probable structure was proposed for complexes shown in a (**Figure 16-19**).

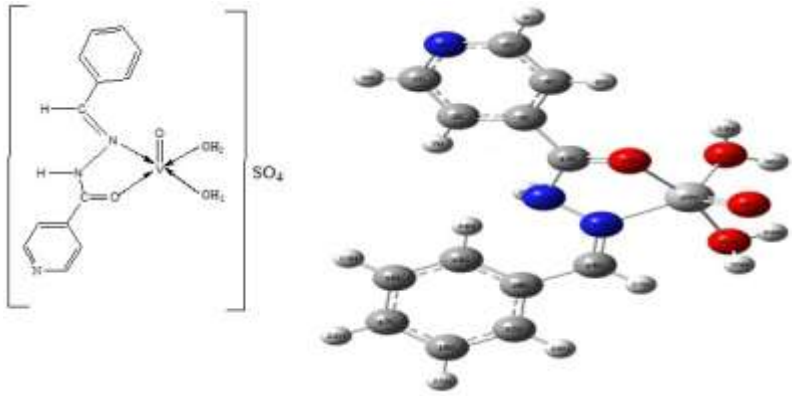

A b

Figure 16: (a) Chemical structure (b) DFT optimized structure of

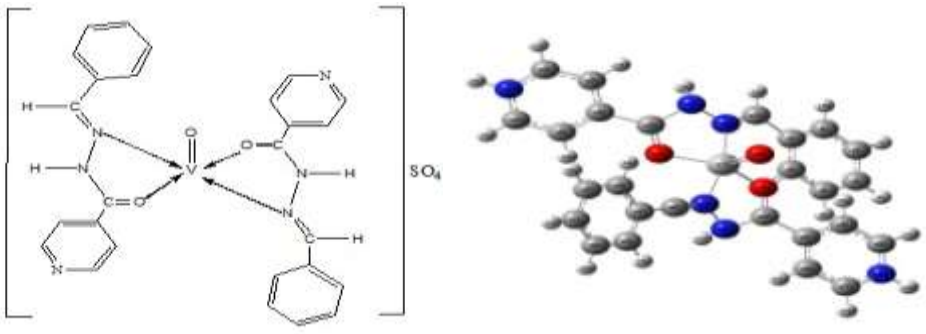

A b

Figure 17: (a) Chemical structure (b) DFT optimized structure of Complex 2

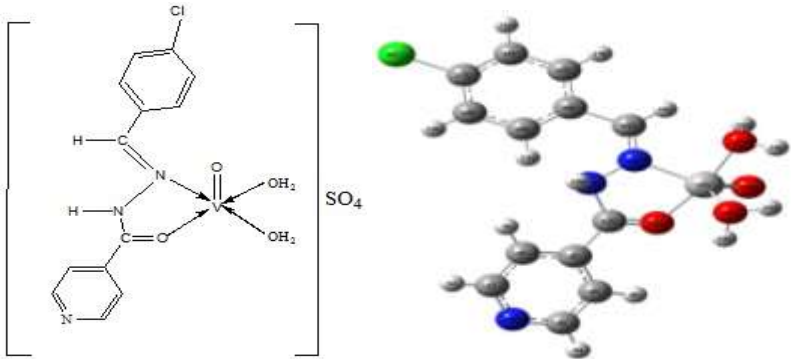

A b

Figure 18: (a) Chemical structure (b) DFT optimized structure of Complex 3

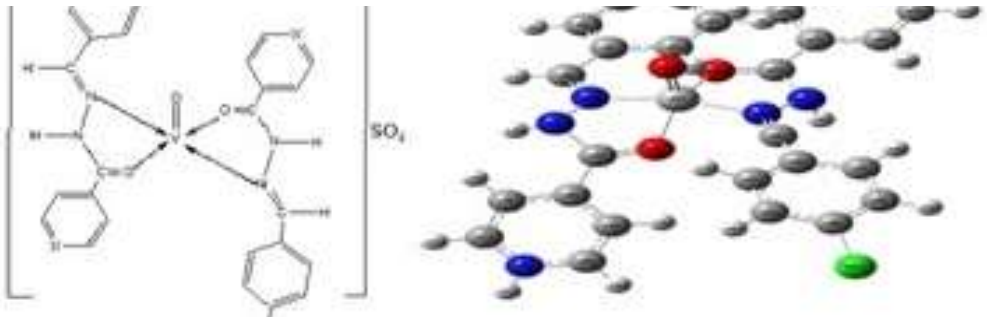

A b

Figure 19: (a) Chemical structure (b) DFT optimized structure of Complex 4

Biological applications

In-Vitro antidiabetic activity

The antidiabetic activity was examined by the standard amylase inhibition assay. Inhibitory activity of synthesized compounds against alpha amylase is shown in **Fig. 20**. All Complexes exhibit more inhibition effectiveness than Schiff base ligands. Complex **1** and **2** show excellent amylase inhibition activity of **66.57 %** and **72.34 %** respectively. However, complex **3** and **4** were show fine activity as compare to ligand.

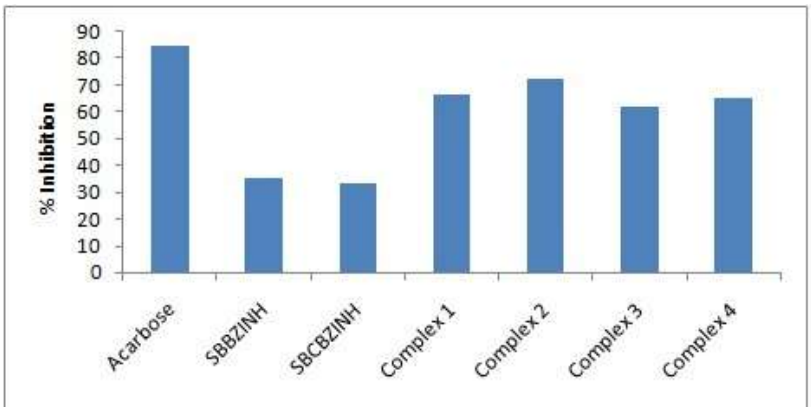

Figure 20: *In-Vitro* antidiabetic study of Ligands and Complexes

Antibacterial Activity

The results of *in vitro* antibacterial activity of all compounds are presented in **Table. 3**. Amoxicillin was used as positive standards and DMSO was used as negative control for this antibacterial activity. Complex **2** displayed highest bactericidal activity against *E. coli* . The other complexes show less activity than complex **2** but greater antibacterial activity than ligand, this may be due to enhanced lipophilicity of the complexes, this leads to the breakdown of permeability barrier of the cell and thus retards the normal cell process in bacteria. The activity order of the synthesized compounds was as follows: **2> 4> 3> 1> L_1>L_2**. The increased activity of metal complexes can also be explained on the basis of chelation theory. MIC is the concentration of the highest dilution tube, in which bacterial growth was absent. It was observed that complex **1-4** has exhibited MIC in between 30-35 µg/mL. The MIC of the complexes also displayed in the table 3.

Table 3: Antibacterial activity of the Ligands and complexes against *E. coli.*

S. No.	Compounds	*Sensitivity	**Diameter of inhibition zone (in mm) MIC concentration, µg/mL
1.	**Standard drug Amoxicillin**	+	48±0.04 -
2.	**L_1**	+	27±0.5 -
3.	**L_2**	+	22±0.3 -
4.	**Complex 1**	+	34±0.5 30
5.	**Complex 2**	+	39±0.6 35
6.	**Complex 3**	+	35±0.8 31
7.	**Complex 4**	+	37±0.5 32
8.	**DMSO**	-	05±0.7 -

*Inhibition zone of more than 8mm was taken as positive (+). **Values as mean ±Standard Error Mean.

Conclusion

Two Schiff bases and their four complexes were synthesized and characterized by spectroscopic techniques. To attain better approach in to molecular structure of compounds some quantum chemical calculations have been performed, *i.e.*, Mulliken charge study, Molecular surface electrostatic potential (MSEP), bond parameters and geometry of complexes was optimized. Synthesized compounds studied for their *in vitro* antidiabetic as well as antibacterial activity. Complex **1** and **2** have exhibited a very promising antidiabetic activity. In view of such promising results, this therapeutic approach may reduces the post prandial glucose level in blood by the inhibition of alpha-amylase enzymes, which can be used as an important strategy in management of blood glucose level. Similarly, all the complexes have displayed good antibacterial activity. Therefore, study of these compounds is quite interesting not only in term of their reactivity but also due to their varied range of activity.

ACKNOWLEDGEMENT

The authors are grateful to **Principal,** Government Science College, Jabalpur and **Head**, Department of Chemistry, for providing necessary laboratory facilities. We sincerely thank **SAIF, CDRI**, Lucknow, for recording ESI-MS, ^{1}H-NMR, ^{13}C-NMR. We are also thankful to Daksh laboratory, Jabalpur for their valuable help of *in-Vitro* Antidiabetic activity. One of us (Sangeeta Jhariya) is also grateful to the UGC-

New Delhi for financial support through RGNF (Award letter no. F1-17.1/2015-16/RGNF-2015-17-SC-MAD-19472/SAIII/Website).

REFERENCES

Becke A D (1993). Density-functional thermochemistry III The role of exact exchange *Journal of Chemical Physics* **98** 5648-5652.

Balachandran V Parimala K (2012). Vanillin and isovanillin: Comparative vibrational spectroscopic studies,conformational stability and NLO properties by density functional theory calculations *Spectrochimica Acta Part A: Molecular and Biomolecular Spectroscopy* ***95***354–368.

Balakrishnan C Neelakantan M A (2017). Crystal Structure and bio-catalytic potential of oxovanadium(IV) Schiff base complexes derived from 2-hydroxy-4-(prop-2-yn-1-yloxy)benzaldehyde and alicyclic/aromatic diamines *Inorganica Chimica Acta* https://doi.org/10.1016/j.ica.2017.09.060.

Djebbar S S, Benali B O and Deloume J P (1998). Synthesis, Characterization, Electrochemical Behavior and Catalytic Activity of Manganese (II) Complexes with Linear and Tripodal Tetradentate Ligands Derived from Schiff Bases. *Transition Metal Chemistry* **23** 443-447.

Dutta R L Syamal A (1993). In Elements of Magnetochemistry 2nd ed., *Affiliated East-West Press New Delhi* 225.

Geary W J (1971). The use of conductivity measurements in organic solvents for the characterisation of coordination compounds. *Coordination Chemistry Reviews* 7 81-122.

Hamada YJ (1997). The Development of Chelate Metal Complexes as an Organic Electroluminescent Material. *IEEE Transition Electron Devices* **44** 1208-1217.

Isaac Z. Gundhla *et. el.* (2014). pH-metric chemical speciation modeling and studies of *in vitro* Antidiabetic effects of *bis*[(imidazolyl)carboxylato]oxidovanadium(IV) complexes. *Journal of Inorganic Biochemistry*.

Jeffery G H Bassett J Mendham J Denney R C and Vogel A.I. (1989). *Textbook of Quantitative Inorganic Analysis, fifth ed.*, 472.

Liu CM, Xiong RG, You XZ, Liu YJ and Cheung KK (1996). Crystal Structure and Some Properties of a Novel Potent Cu_2Zn_2 SOD Model Schiff Base Copper (II) Complex. *Polyhedron* **15** 4565-4571.

Lee C Yang W Parr R G (1988). Development of the Colic-Salvetti correlation-energy formula into a functional of the electron density *Physical Review. B, Condensed Matter and Materials Physics* **37** 785-789

Mazzola PG, Jozala AF, Novaes LCL, Moriel P and Penna TCV (2009). Minimal Inhibitory Concentration (MIC) Determination of Disinfectant and/or Sterilizing Agents. *Brazilian Journal of Pharmaceutical Science* **45**(2) 241-248.

Mir J M Mir RajakD K and Maurya R C (2017). Bacterial sensitivity and SOD behavior of N-pyrone glucosamine Schiff base Fe(III) complex: Conjoint experimental-DFT evaluation *Journal of Coordination Chemistry* **70** 3199-3216.

Mehrotra R Shukla S N and Gaur P (2011). Spectroscopic characterization of Schiff base coordinating monomolecular trinuclear complexes prepared through tailored synthesis. *Journal of Coordination Chemistry* 1–15.

Maurya R C Malik B A Mir J M and Sharma A K (2014). Synthesis, characterization, thermal behavior, and DFT aspects of some oxovanadium(IV) complexes involving ONO-donor sugar Schiff bases. *Journal of Coordination Chemistry*, **67(18)** 3084–3106.

Pelczar MJ, Chan ECS and Krieg NR (2001). *Text Book of Microbiology*, 5th edition (McGraw-Hill Publishing Company Limited) New Delhi, India 138.

Raj P S Shoba D Ramalingam S Periandy S (2015). Spectroscopic (FT-IR/FT-Raman) and computational (HF/DFT) investigation and HOMO/LUMO/MEP analysis on 1, 1-difluoro-2-vinylcyclopropane *Spectrochim. Acta Part A* **147** 293-302.

R Amit YAUL B Gaurav PETHE and S Anand ASWAR (2014). Synthesis, Characterization and Catalytic studies of some oxovanadium(iv) complexes of tetradentate Schiff base ligands *Revue Roumaine de Chimie* ***59*****(1)** 15-26.

Sahani MK, Pandey SK, Pandey OP and Sengupta SK (2014). A series of novel oxovanadium(IV) complexes: Synthesis, spectral characterization and antimicrobial study. *Journal of Molecular Structure* **1074** 401-407.

Samy M. El-Megharbel, Reham Z. Hamza, Moamen S. Refat (2015). Synthesis, spectroscopic, structural and thermal characterizations of vanadyl(IV) adenine complex prospective as antidiabetic drug agent. *Spectrochimica Acta Part A: Molecular and Biomolecular Spectroscopy* **135** 850–864.

Shukla S N, Gaur P, Gupta J.P, Mathews S and Rai N (2015). Synthesis, Characterization and Antibacterial activity of Complexes of Palladium with Schiff bases derived from 1, 3-diaminopropane. *International Journal of Basic and Applied Chemical Sciences* ***5 (1)*** 18-28.

Shivakumar L, Shivaprasad K and Revanasiddappa HD (2012). Synthesis, spectroscopic characterization, antimicrobial, DNA binding and oxidative-induced DNA cleavage activities: New oxovanadium(IV) complexes of 2-(2-hydroxybenzylideneamino)isoindoline-1,3-dione. *Spectrochimica Acta Part A: Molecular and Biomolecular Spectroscopy* **97** 659–666.

Shoba D Periandy S Karabacak M and Ramalingam (2011). Vibrational spectroscopy (FT-IR and FT Raman) investigation, and hybrid computational (HF and DFT) analysis on the structure of 2,3-naphthalenediol. *Spectrochimica Acta Part A: Molecular and Biomolecular Spectroscopy* **83** 540– 552.

Silavwe H N Villa Rodriguez J A Ifie I Holmes M Aydin E Jensen J M Williamson G (2015). Inhibition of human α-amylase by dietary polyphenols. *Journal of Functional Foods* **19** 723 732.

Shukla S N Gaur P Mathews S khan S and Srivastava A (2008). Synthesis characterization catalytic and biological activity of some bimetallic selenocyanate Lewis acid derivatives of N, N0-bis(2 chlorobenzylidene)ethylenediamine. *Journal of Coordination Chemistry* **61**, 3913–3921

Sachin S W and Narayan S B(2012). Microwave Assisted Synthesis and Antioxidant Activity of Vanadium(IV) Complexes of Amino Acid Schiff Bases. *Synthesis and Reactivity in Inorganic Metal-Organic and Nano-Metal Chemistry* **42**1098–1104.

Tyagi P Sulekh Chandra S Saraswat B S and Yadav D (2015).Design, spectral characterization, thermal, DFT studies and anticancer cell line activities of Co(II),Ni(II) and Cu(II) complexes of Schiff bases derived from 4-amino-5-(pyridin-4-yl)-4H-1,2,4-triazole-3-thiol. *Spectrochimica Acta Part A: Molecular and Biomolecular Spectroscopy* **145** 155–164.

Zhang S (2017). Crystal structure and NMR study of a bis-peroxovanadium complex [NH4][VO(O2)2(ima)] *Journal of Coordination Chemistry* **70(17)** 1-21.